Aligning the Thomson Scattering and Charge Exchange Recombination Diagnostics Using Neutral Beam Emission at DIII-D

Abigail Feyrer,[1, a)] S.R. Haskey,[2] C. Chrystal,[3] and C.A. Aidala[4]
[1)] *Plasma Science and Fusion Center, Massachusetts Institute of Technology, Cambridge, Massachusetts, 02139, USA*
[2)] *Princeton Plasma Physics Laboratory, Princeton, New Jersey 08543-0451, USA*
[3)] *General Atomics, P.O. Box 85608, San Diego, California 92186, USA*
[4)] *University of Michigan, Ann Arbor, Michigan, 48109, USA*

(Dated: 28 March 2024)

This work addresses discrepancies in the alignment of the H-mode pedestal profiles of the electron and ion properties in the DIII-D tokamak as measured by the Thomson Scattering (TS) and the Charge Exchange Recombination Spectroscopy (CER) diagnostics. While alignment of these profiles is key for accurate studies of tokamak physics and plasma confinement, misalignments can occur due to inaccuracies, such as in magnetic equilibrium reconstructions required to map measurements in different poloidal and toroidal locations. Both FIDASIM, an established simulation package, and a simplified collisional radiative model are used to simulate neutral beam state densities and neutral beam emission. Simulated neutral beam emissions are calculated based on shifted TS profiles and compared to beam emission measurements from the Main Ion CER system to determine the best shift for aligning TS with CER. This analysis is performed on various DIII-D discharges.

I. INTRODUCTION

The DIII-D tokamak[1] is a device built to study controlled fusion. Several key measurements in DIII-D are of ion and electron temperature and density profiles, which are important for analysis of pedestal stability[2], transport, and confinement[3]. Impurity ion temperature, density, and rotation are measured by the charge exchange recombination (CER) diagnostic[4,5], while electron density and temperature are measured by the Thomson scattering (TS) diagnostic[6]. Unfortunately, CER and TS measure quantities at different toroidal and poloidal locations within the DIII-D tokamak. Magnetic flux coordinates such as the square root of the normalized toroidal flux (ρ), which is defined to be 0 at the magnetic axis of the plasma and 1 at the separatrix, allow measurements of CER and TS to be mapped together based on one parameter. These coordinates are typically based on a magnetic equilibrium calculated by EFIT[7] and the assumption of fast equilibration of plasma densities and temperatures within a flux surface. However, there is uncertainty in this mapping, especially near the plasma edge in the region known as the pedestal[3], where small deviations from assumed symmetry can cause large errors in alignment due to steep gradients in the profiles. This work seeks a better way to compare electron and ion measurements and improve alignment between their profiles.

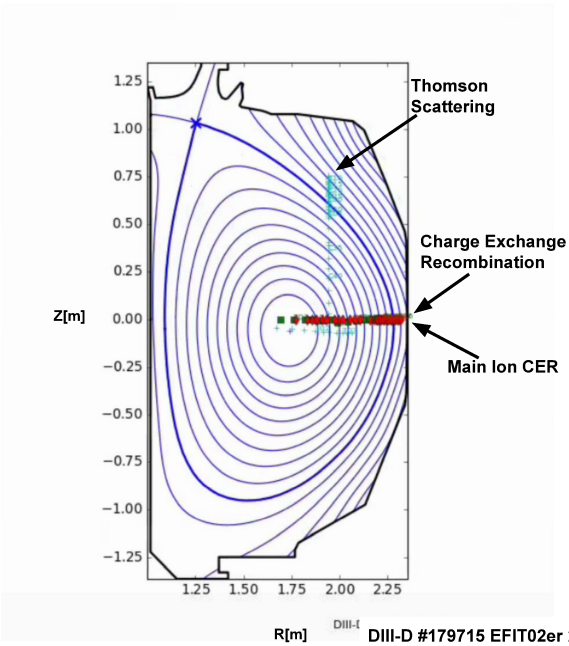

FIG. 1. Viewing chords of TS, CER, and MICER diagnostics. Differences in both the poloidal and toroidal locations of TS and CER lead to uncertainty in mappings between their measurements.

The Main Ion CER diagnostic (MICER)[8,9], measures Balmer-α emission from neutral deuterium. When viewing a neutral beam injection (NBI), this spectrum contains information about deuterium ion density, temperature, and rotation due to charge exchange with the neutral beam, as well as emission from the neutral beam itself. MICER and CER sight lines are interwoven with each other (See Fig. 1 in Grierson 2016[10]), which makes the relative position of their measurements fixed. Unfortunately this is not possible when comparing them to TS data, due to its different toroidal and poloidal locations. See FIG.1 for the location of various measurements. This means that to compare TS and CER measurements one must use their mappings to ρ as calculated by EFIT, which assumes axisymmetry. Misalignment between measurements is possible due to uncertainty in the input measurements used to constrain EFIT, error in the equilibrium reconstruction provided by EFIT, or 3D effects which break

[a)] Electronic mail: feyrer@mit.edu

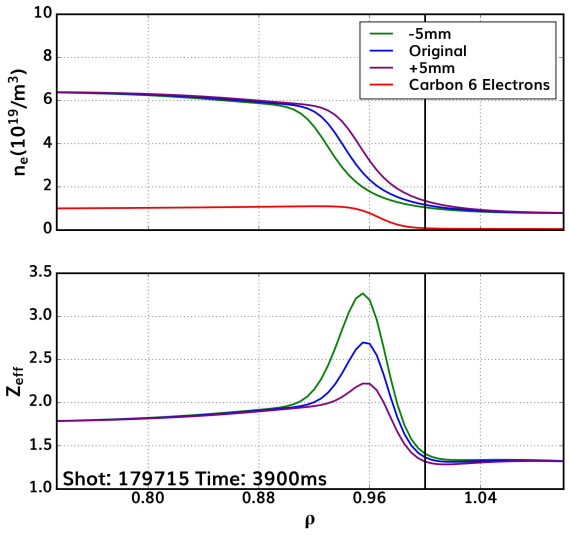

FIG. 2. Electron and 6× carbon 6+ densities plotted together to show the effects of potential misalignment. Shifting the electron density by just ±5mm (The uncertainty within EFIT) changes the effective nuclear charge (Z_{eff}) drastically. The peak of the Z_{eff} spike at the edge changes from 3.2 to 2.2 within the EFIT uncertainty range.

assumed symmetries. This broken symmetry may be due to known errors in the position of the field coils[11] or ripple due to a finite number of toroidal field coils, which can make EFIT reconstructions inaccurate for certain toroidal locations. Misalignment is known to be a problem due to certain extreme cases where comparison of measurements leads to unphysical results such as breaks from quasi-neutrality. These compounded uncertainties can lead to up to a cm or more shift in extreme cases. An example of a case with potential misalignment is shown in FIG.2. The electron density from TS and carbon ion density from CER are used to construct effective nuclear charge (Z_{eff}) profiles. Though other impurity species may be present, calculation of Z_{eff} here only uses the CER and TS data because carbon is the dominant intrinsic impurity in DIII-D due to the carbon walls. Z_{eff} profiles are very susceptible to misalignment between TS and CER data. Shifting the TS profiles by just ±5mm, or the generally accepted EFIT uncertainty, drastically changes the Z_{eff} profile, as can be seen in FIG.2.

Misalignment between diagnostic measurements can limit analysis that requires both electron and ion properties. Parameters such as Z_{eff} , total pressure gradient, bootstrap current, or heat fluxes become much more uncertain when correct alignment is unknown, especially around the pedestal edge of the plasma. To solve these problems there are existing ways of aligning TS and CER measurements. One such method uses a two-point model to calculate expected separatrix temperatures consistent with thermal conduction to the target plates[12]. These temperatures are typically around 80 eV at DIII-D[13]. These methods tend to improve alignment compared to raw profiles, but contain uncertainty in and of themselves, as they are based only on rough rules for plasma properties at the separatrix. This uncertainty can limit the scope of analysis done with these profiles, and better alignment methods based on experimental measurements would improve investigations of pedestal transport and stability that rely on accurate profiles in the pedestal edge region.

Among the parameters measured by MICER, the full energy neutral beam emission (BE) allows for a new alignment method which can reduce uncertainty in derived quantities that are calculated from both electron and ion profiles. This is because the BE is related to electron density through the impact excitation process that populates the excited state responsible for the emission. Conveniently, BE can be simulated using inputted plasma temperature and density profiles. This means that simulation and MICER measurement of BE can be used to improve alignment between TS and CER.

In order to extract the BE measurement from the MICER spectra a fitting tool is used. The full details on how this can be done are found in Haskey 2018[9], but a simpler process which does not require the use of the FIDASIM simulation code[14,15] is typically used for routine shot analysis. Emission from the neutral beam is split into three parts: the full(D^+), half (D_2^+), and third (D_3^+) energy which are accelerated to differing velocities. Within each beam energy, there are 9 significant components from Stark splitting whose wavelength shifts and intensity ratios can be calculated from atomic physics. A least squares minimization fit then determines the total intensity of all of these components using these constraints. Within this process, photon statistics and read noise are used to assign an error to each point in the spectrum, and the overall error in a single BE intensity measurement is found by taking the diagonal elements in a covariance matrix. This work uses the full energy BE exclusively as there is less uncertainty in the measurement. Further, as will be later discussed, measurements of the full energy BE over a short time window are used for the alignment procedure, and the population standard deviation of these measurements is used as a way to encompass both the underlying measurement uncertainty and uncertainty associated with small variations in plasma parameters.

II. BEAM EMISSION THEORY

The rate of neutral beam emission is directly proportional to the density of neutrals with electrons in the appropriate excited state. For the Balmer-α line ($n = 3 \rightarrow 2$) this would be proportional to electrons in the n = 3 state. To calculate beam emission, one must thus calculate the neutral state densities as beams move into the plasma. This can be effectively modeled using two main processes: collisions of the beam neutrals with plasma particles and spontaneous decay. Simulations of this sort are called collisional radiative models, and more information on them can be found in Hutchinson, 2002[16]. Collisions can cause excitation, de-excitation, charge exchange, and ionization of neutrals. This is further complicated by the fact that there are several types of particles to collide with in the plasma: electrons, deuterium ions, and various impurity ions.

Each energy level change for collisions with each species has a different cross section which depends on the relative velocities between the species, and thus depends on species temperature. These dependencies are built into atomic physics rates which are then multiplied by relevant densities to get process rates. Rate equations for a single state with all relevant processes can be written as:

$$\begin{aligned}\frac{df_n}{dt} &= -(\sum_{k=i,Z} f_n d_k X_n^k + \sum_{k=e,i,Z} f_n d_k I_n^k) \\ &+ \sum_{m>n}(f_m A_{m\to n} + \sum_{k=e,i,Z}(f_m d_k q_{m\to n}^k - f_n d_k q_{n\to m}^k)) \\ &+ \sum_{n>m}(-f_n A_{n\to m} + \sum_{k=e,i,Z}(f_m d_k q_{m\to n}^k - f_n d_k q_{n\to m}^k))\end{aligned} \quad (1)$$

Here f_n represents the density of neutrals in state n, d_k represents the density of species k, and e, i, and Z represent electrons, main ions, and impurities respectively. X_n^k represents the cross section of charge exchange to species k from state n, and I_n^k represents the ionization cross section from state n due to a collision with k. $A_{m\to n}$ is the Einstein coefficient which governs the rate of emission from state m to n, and $q_{m\to n}^k$ represents the cross section of excitation or de-excitation from state m to n due to a collision with species k.

Rate equations for all states can be written in matrix form:

$$\begin{pmatrix} df_1/dt \\ df_2/dt \\ . \\ . \\ . \\ df_{n_{max}}/dt \end{pmatrix} = \begin{pmatrix} a_{11} & a_{12} & ... & a_{1n_{max}} \\ a_{21} & a_{22} & ... & a_{2n_{max}} \\ . & . & & . \\ . & . & & . \\ . & . & & . \\ a_{n_{max}1} & a_{n_{max}2} & ... & a_{n_{max}n_{max}} \end{pmatrix} \begin{pmatrix} f_1 \\ f_2 \\ . \\ . \\ . \\ f_{n_{max}} \end{pmatrix} \quad (2)$$

Here, a_{mn} is a summation of all process rates that would cause a neutral to transition from state m to state n. a_{nn} is the sum of all processes that would cause a neutral to transition out of state n, which includes transitions to other states as well as charge exchange and ionization. Diagonal elements are always negative, as density increases cannot come from the same state. n_{max} is chosen based on the desired accuracy of the model, but tracking up to $n = 6$ is often used due to availability of cross sections. Typically, it is convenient to write these equations in terms of space rather than time using the velocity of the neutral beams and $x = vt$.

Because of the spatially varying parameters, this matrix equation can be solved by discretizing in space, iterating across the plasma, and updating each state density with each step into the plasma. This starts at the edge and can be iterated all the way through the tokamak. With each step, neutral state densities are updated, and these updated densities are used for the next step. Beam emission (BE) can then be calculated integrating the density of neutrals in the $n = 3$ state across the lines of sight (LOS) of measurement devices using the equation:

$$BE = \frac{A_{32}}{4\pi}\int_{LOS} f_3(x,y,z)\cdot dl_{LOS} \quad (3)$$

An example of a simulation code that uses a collisional radiative model is FIDASIM. FIDASIM (Fast Ion Deuterium Alpha Simulation) is a Monte Carlo simulation code which takes in tokamak density and temperature profiles and uses them to simulate various diagnostic measurements including neutral beam emission[14,15]. This code has been designed for use on a variety of tokamaks including DIII-D, and can simulate the results of several diagnostics including MICER. A Monte Carlo collisional radiative model is used to calculate neutral state densities by launching many test particles. FIDASIM only tracks atomic states from $n = 1$ to $n = 6$ due to availability of rate coefficients. Process rates can be found in a look-up table or calculated as needed from the cross sections. Matrix coefficients are then found by summing over the relevant rates. The matrix equation is solved analytically via matrix exponentiation, which is used to advance the densities as a track moves through the plasma. This is done to determine densities of various states at any given position. For this alignment method, FIDASIM's calculation of the beam Balmer-α emission is of interest as it is the quantity that is compared with measurements from MICER. The Balmer-α emission from each cell can be found by multiplying the density of neutrals in the $n = 3$ state by the Einstein coefficient, A_{32}. Using line of sight geometries, the predicted spectra for diagnostics can be found from identifying the amount of light that reaches the lenses along with the appropriate Doppler shifts due to the neutral velocity, and splitting due to the motional Stark Effect. FIDASIM's model has been verified through comparisons to several diagnostics on several different tokamaks[15].

III. ALIGNMENT USING BEAM EMISSION

The alignment process works as follows: TS profiles are shifted in relation to CER profiles, beam emission is simulated from these shifted profiles, and the simulation results are compared to MICER measurements. Within this process the main ion density profiles used for simulations are calculated from electron and carbon 6+ density profiles using quasineutrality. In principle, shifting electron density profiles can affect calculation of CER profiles due to beam attenuation. However, in this region attenuation is low, so small changes in beam attenuation with shifts of the electron density are ignored. In comparing the different shifts, a reduced χ^2 (χ^2_{red}) metric is used to evaluate and quantify which shift best lines up with measurements. The shift with the lowest χ^2_{red} is applied to TS measurement and used to align profiles. χ^2_{red} is calculated only from the steep gradient region of measurements, as this is where misalignment has its largest effects. The standard deviation of multiple measurements over a reasonably stationary time period (typically between 50 and 100ms) is used as the error for the χ^2_{red} metric. Note that TS profiles are shifted to CER measurements because those measurements are made next to a poloidal array of Mirnov magnetic probes used in the equilibrium reconstruction, so it is assumed that the relationship between the reconstructed separatrix and the CER measurements is quite good. There is also known misalignment of poloidal field coils near the TS system[11], adding additional

TS ρ Shift	-0.030	-0.025	-0.020	-0.015	-0.010	-0.005	0.000
χ^2_{red}	12.754	10.455	4.935	2.340	0.742	0.323	0.773

TABLE I. χ^2_{red} as a function of TS ρ shift for simulated beam emission compared to MICER measured beam emission. This analysis is performed on discharge 185838 at a time of 3400ms, and -0.005 is determined to be the best shift as it has the lowest χ^2_{red} .

uncertainty in the determination of the separatrix locations near the TS measurements. While this method is primarily focused on aligning TS and CER measurements to each other and does not seek to align them with the correct separatrix location, the decision to shift TS rather than CER data was made to potentially improve TS alignment with the separatrix.

A. Alignment using 3D Monte Carlo collisional radiative model

Initially, FIDASIM was used to simulate neutral beam emission and perform this alignment. Scans of seven simulations, each at increments of 0.005 in ρ from each other are compared to measurements. χ^2_{red} is compared to determine which shift is best, with a resolution of ± 0.005 in ρ. After finding the best shifts, separatrix temperatures within scans are compared.

This analysis was performed on three plasma discharges: 185838, 183235, and 179715. This initial data set was selected because high quality MICER analysis was available for all the discharges. These discharges are all in H-mode with T_e values of around 3.5keV at the top of the pedestal. 185838 and 185235 are both lower single null plasmas while 179715 is upper single null, and electron densities range from around $6.5 \cdot 10^{19} m^{-3}$ in 179715 and 183235 to up to $11 \cdot 10^{19} m^{-3}$ in 185838 at the top of the pedestal. B_t was between 2 and 2.1 T and plasma current was around 1.3 MA for all three discharges. Profiles for these discharges generally exclude times with edge localized modes (ELMs). ELMs are instabilities present in H-mode plasmas that can cause fractions of plasma energy to be rapidly released[17]. The brightness normalization function described later in Section IV was not used in the FIDASIM analysis of these shots. Results showed that alignment was necessary, as unshifted simulations typically did not line up best with MICER measurements in comparison with shifted simulations. A χ^2_{red} metric is used to find the profile which matches best with measurement, and results can be confirmed by inspecting plotted profiles. An example of these alignment results and values for discharge 185838 at time 3400ms can be found in FIG.3 and Table I. FIG.3 provides the shifted and simulated emissions in comparison with measurements, as well as the shifted TS data and Z_{eff} . In Table I the calculated χ^2_{red} is shown for each shift, revealing -0.005 as the shift with the lowest χ^2_{red} , and therefore the best shift. By eye in FIG.3 this shifted emission agrees well with measurements. The best shift does however have a small dip in Z_{eff} near the edge which may be due to lower charge state carbon ions near the edge of the plasma. However, the dynamics of Z_{eff} and impurities around the edge of the plasma are largely uncertain, making it difficult to draw conclusions from this single result.

When plotting χ^2_{red} for each scanned simulation across one discharge (FIG.4), the optimum shift varies with time. Even between times as close as 100ms, the best shift changes. However, when plotting χ^2_{red} vs. electron temperature at the separatrix in the shifted TS profiles across a discharge, the relation stays much more fixed across different times. For discharge 185838, the best shift separatrix temperature hovered around 55eV. This is lower than the typically expected value of 80eV mentioned earlier. This may be due to remaining uncertainty in the location of the separatrix, as this method only seeks to align TS and CER with each other and does not necessarily align them with the separatrix. EFIT has an uncertainty on the order of mm, and the shift of -0.005 in ρ corresponds to a physical shift of 2.5mm at the midplane which is consistent with this uncertainty. The relatively constant nature of the separatrix T_e is as expected, as separatrix T_e likely should not change over the course of discharges that are running with stationary conditions.

B. Rapid alignment using 1D simplified model

FIDASIM produces results that are comparable to MICER data and uses sophisticated and accurate modelling techniques. However, each FIDASIM run takes about 3 minutes due to its complexity and the overhead required to run the simulation. Aligning TS and CER requires between 7 and 15 simulations per individual timeslice to perform a scan of TS ρ shifts and evaluate which shift lines up best with MICER measurements. Each discharge could be split into tens of timeslices, making FIDASIM too computationally expensive for routine discharge alignment. Thus, we created a simplified collisional radiative model which requires less time to compute a result. This code relies on FIDASIM's framework for taking in relevant data, and uses the same coordinate system as FIDASIM to simplify model startup. This simplified model is coded with the goal of producing fast beam emission simulations similar to FIDASIM's.

The simplified collisional radiative model simulates the neutral beam in one dimension. The beam travels along the center of the beamline, which is taken as the $\hat{x}$ direction. A coordinate system with $\hat{z}$ being vertical and $\hat{y}$ being the remaining direction in a right handed coordinate system is used for this simulation. In these coordinates the one dimensional beam travels at what would be $y = z = 0$. Profiles along this line are used to calculate excitation, ionization, and charge exchange cross sections, and similar to FIDASIM, the model iterates into the plasma, updating densities as it goes. This one dimensional simulation is then used to calculate the state densities everywhere. The initial conditions for each (y,z) point are determined using the geometry of the neutral beam injection (NBI) which is typically specified as a Gaussian in the y and z directions. The f_3 density is then interpolated onto the (x,y,z) grid by using the ρ values at each location along the grid. The emission is then calculated using Eqn.3.

When compared across all timeslices in a discharge, this

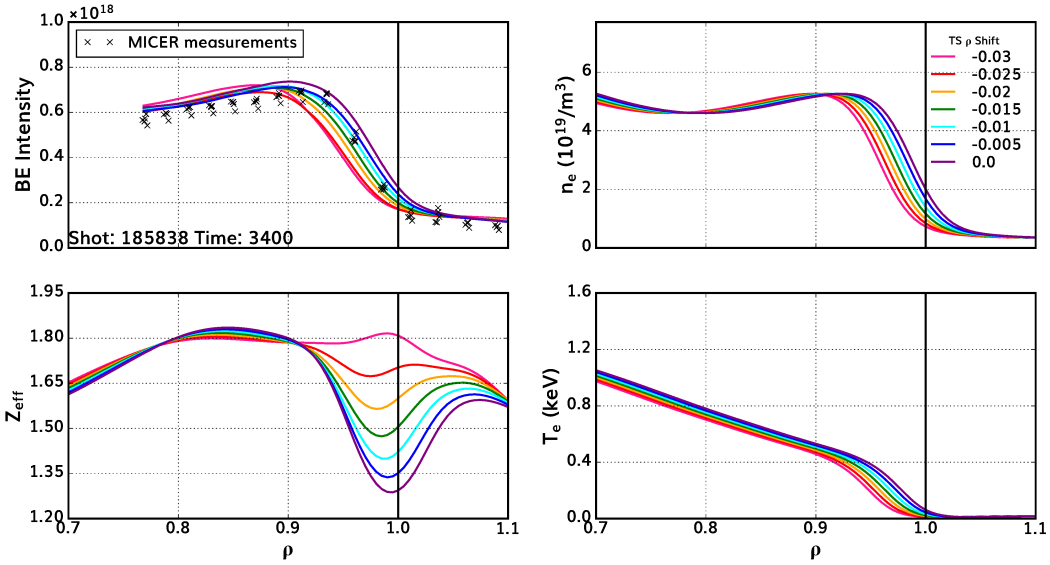

FIG. 3. A FIDASIM scan on discharge 185838 time 3400 ms. TS density and temperature profiles (upper and lower right respectively) are shifted and beam emission is simulated using FIDASIM (top left). Note that the normalization method described later in Section IV is not used here, as simulations show good agreement with measurement. Z_{eff} is also calculated from shifted profiles and presented (lower left), as it is strongly affected by misalignment. A best shift can be determinedwith χ^2_{red} and for this timeslice -0.005 agrees best with measurement.

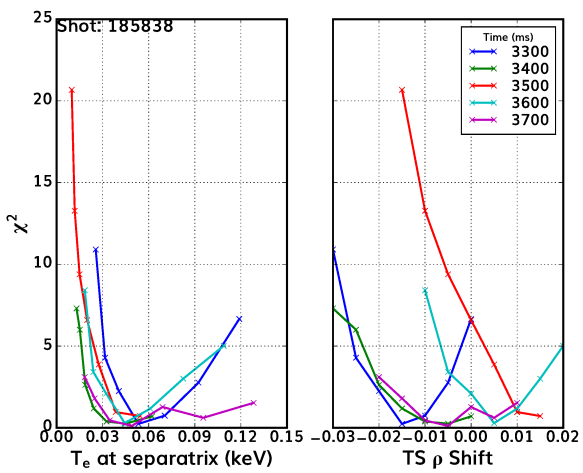

FIG. 4. Comparing χ^2_{red} values across ρ shift scans for discharge 185838. χ^2_{red} are presented as a function of separatrix T_e and TS ρ shift. While best ρ shift moves around over the course of a discharge, separatrix T_e remains relatively constant at around 55eV.

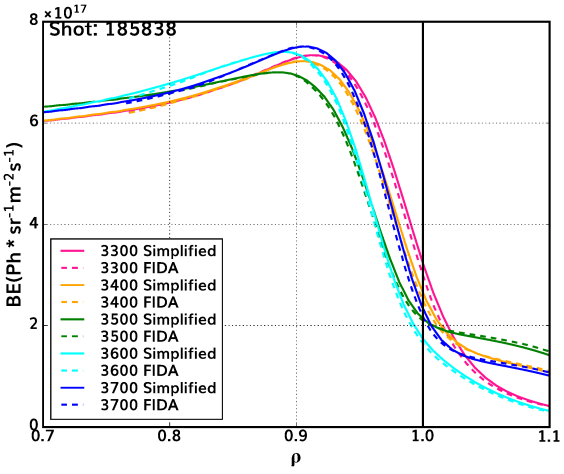

FIG. 5. The 1D beam emission simulation compared with FIDASIM's across times (in ms) in discharge 185838. Simulations have been scaled to match FIDASIM's maximum intensity to emphasize differences in ρ rather than magnitude. The 1D method matches FIDASIM well.

method matches FIDASIM relatively well. FIG.5 shows the close agreement between FIDASIM simulated beam emission and the fast model beam emission. It is important to use ρ values for interpolation because the beam injection angle is not perpendicular to flux surfaces meaning that one x value corresponds to a range of ρ values depending on the y and z location. The change in excited state densities depends on plasma parameters at a given point which are constant along constant ρ values which is why ρ is used for interpolation rather than x. Due to its speed and relative accuracy, this new

interpolation method based on 1D density is used for alignment along with an optimizer to find the shift that minimizes χ^2_{red} .

IV. BRIGHTNESS NORMALIZATION FUNCTION

For this alignment method, the shape of the beam emission profile and position of the steep gradient region are what matter for accurate alignment. For some discharges, the profiles calculated with FIDASIM or the simplified model can differ from the measurement in a systematic way. These differences could be caused by an error in the beam power, beam energy fractions, or a systematic error in the electron or deuterium density. There are challenges associated with each of these measurements that cannot be resolved here, but as the location of the steep gradient region is not affected by these errors, it was found that applying a brightness normalization was sufficient to enable good alignment results to be extracted from the data. Note that the light sensitivity of the MICER diagnostic is calibrated between experimental campaigns with a calibrated integration sphere, and the errors in question vary considerably between discharges in a way that is not easily explained by an error in the diagnostic sensitivity. For this reason a constant multiplier is incorporated into the simulation to effectively normalize the simulation and measurements to each other.

Several methods for applying a multiplier were tested by performing ρ shift scans using the simplified beam emission model and observing the results. Method 0 (and the method used in FIG.6) takes the maximum measured emission value, and scales simulated emission to match it, using the equation $m = max(BE_{measured})/max(BE_{sim})$ where m is the multiplier. Note that MICER data used for this is time averaged over a range typically between 50 and 100 ms. Methods 1-3 all minimize χ^2_{red} by varying m. Method 1 minimizes χ^2_{red} only in the pedestal top region, method 2 uses the entire range of MICER data, and method 3 does this in the high gradient region. Methods 0-2 all performed similarly, provided similar agreement with measurement and determined similar best shifts. Method 3 on the other hand, varied significantly in its agreement with measurement depending on ρ shift applied. Since methods 0-2 have similar agreement to measurement and determine similar best shifts, method 0 is now the default method used and results using this method on discharge 182703 are shown in FIG.6.

V. ALIGNMENT RESULTS

Discharge alignment was performed using a least squares optimizer from scipy[18] to find the shift that minimizes χ^2_{red} using the fast beam emission simulation. This analysis was performed on a variety of discharges, but 185838 is presented here as results can be compared with FIDASIM's alignment shown in the previous section. An example of this alignment determination process run on discharge 185838 for time 3400ms can be found in FIG.7. The emission calculated with

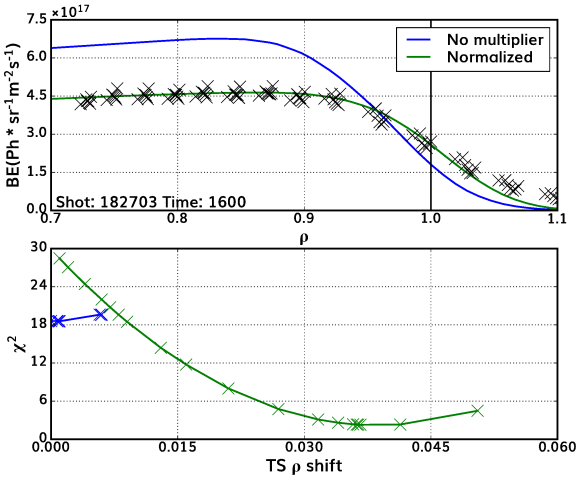

FIG. 6. Comparison of best shifts found both with and without a normalizing multiplier applied to beam emission simulations. The top graph shows the discrepancy in the magnitude of measurements versus simulations without a multiplier, while the bottom graph shows results of using a χ^2_{red} optimizer on simulations both with and without a multiplier applied. With a multiplier, simulated emissions match measurement better and a clear ρ shift minimum is found.

a shift of -0.008 agrees better than the unshifted emission with MICER measurement, and a clear minimum in χ^2_{red} is found.

In comparing electron separatrix temperature across shifted simulations, the separatrix temperature appears more variable than it did from FIDASIM simulations. This variance is likely due to the uncertainty of 0.005 ρ from the step size in the FIDASIM alignment or the slight difference between FIDASIM and the simplified beam emission simulations. Similarly to FIDASIM, the best shift still varies throughout a discharge. This variance across time can be seen in FIG.8. The brightness normalization function was used in this analysis and multipliers found to be around 0.8 are applied to each simulation for each time in this discharge.

Analysis was performed on six discharges with varying characteristics, and the alignment results for the spatial Thomson shift are presented in FIG.9. These discharges span electron densities from $4.5 - 11.2 \cdot 10^{19} m^{-3}$, and electron temperatures from $2.1 - 2.5$keV at the top of the pedestal. Magnetic fields range from 1.75-2.1T and plasma currents range from 1.1 to 1.3 MA. Discharges 184833 and 184969 are both QH-mode while the rest are H-mode. Discharges 182725 and 182703 are upper single null while the rest are lower single null. While MICER profiles always exclude times with ELMs, shots 182725 and 182703 do not have ELM times removed in their TS and CER profiles. In this analysis normalization multipliers ranged from 0.5 to 0.95. Over the course of each discharge the best shift varies by 1-2cm, while the largest shift found was around 4cm. These differences could be due to EFIT uncertainty or the known misalignment of various coils in the tokamak[11] which could cause varying misalignments

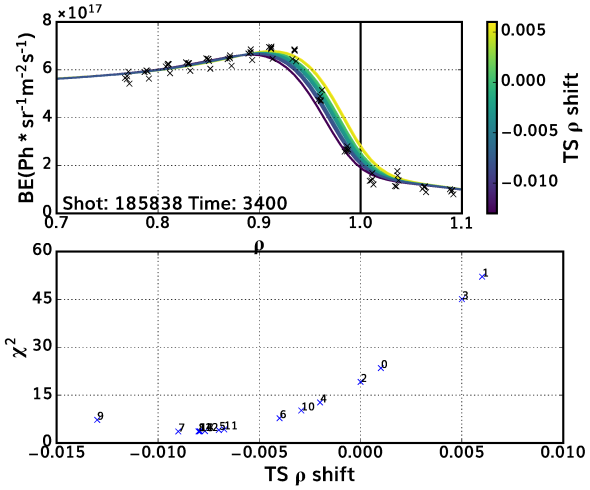

FIG. 7. Using scipy.optimize's least_squares function to find the lowest χ^2_{red} and therefore best TS ρ shift for discharge 185838 at time 3400ms. Calculated shifted beam emissions are shown in the top plot and compared to MICER data. χ^2_{red} for each emission simulation is shown in the bottom plot revealing the best shift which for time 3400ms is found to be -0.008.

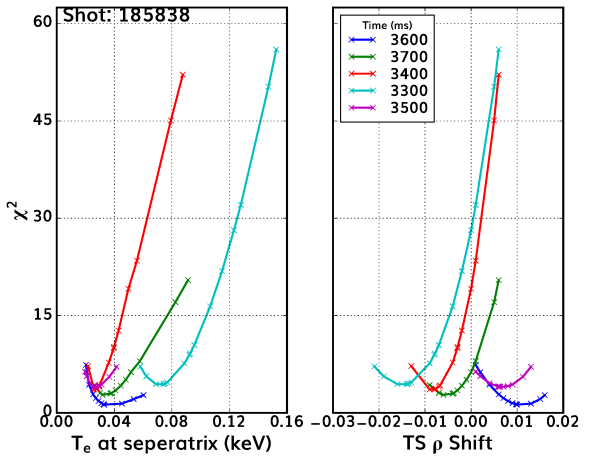

FIG. 8. Comparing χ^2_{red} values from fast beam emission simulations across various ρ shifts for discharge 185838. χ^2_{red} are presented as a function of separatrix T_e and TS ρ shift. The relation between χ^2_{red} and both of these parameters varies over the course of the discharge.

discharge to discharge due to differing currents in the coils.

VI. CONCLUSIONS AND FUTURE WORK

A novel method to address the problem of misalignment between measurements from the Thomson Scattering and

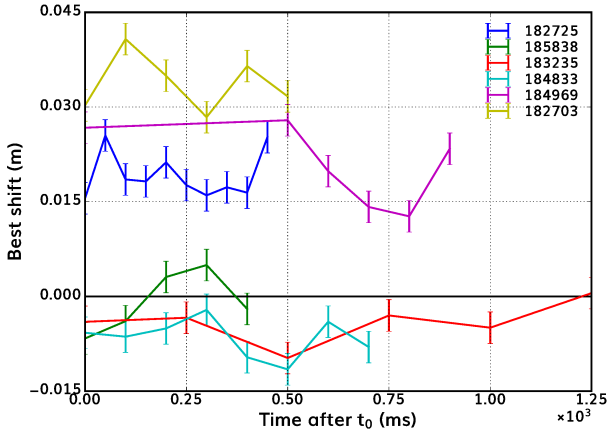

FIG. 9. Best shift as determined by the alignment method for various discharges across various times. For each discharge t_0 is the earliest timeslice for which alignment is performed. Best shift varies over the course of each discharge by a couple of cm, but can vary much more discharge to discharge.

Charge Exchange Recombination diagnostics at DIII-D has been described. Simulations of neutral beam emission are made using shifted TS profiles and compared to MICER measurements to determine the best shift for alignment. This was initially done using FIDASIM, but a 1D collisional radiative model was developed to simulate beam emission faster. This model interpolates densities onto a 3D-grid using magnetic flux coordinates (ρ). This simplified model matches FIDASIM relatively well with faster computation, making it possible to simulate beam parameters accurately in 1 dimension. Using this simulation method on shifted TS profiles along with an optimizer allows for fast determination of best shift with a resolution of about 0.005 in ρ. The alignment method developed is grounded in reasonable physical modeling and has been shown to be viable for routine discharge analysis due to its speed. Results improve upon existing methods which typically rely on ad-hoc assumptions due to lack of measurements to assist in alignment. This method provides a mapping between measurements from CER and TS, but leaves uncertainty in the mapping between measurements and ρ coordinates.

Through alignment of multiple times in several discharges, it was determined that absolute ρ shift typically varies across a discharge, and even on timescales as low as 100 ms. This is likely due to physical shifts in the location of the separatrix over the course of the discharge. Performing this method on many discharges could provide a variety of results and future scientific work could use these results to come up with a physical explanation for the cause of the shifts.

ACKNOWLEDGMENTS

This material is based upon work supported by the U.S. Department of Energy, Office of Science, Office of Fusion Energy Sciences, using the DIII-D National Fusion Facility, a DOE Office of Science user facility, under Awards DE-FC02-04ER54698 and DE-AC02-09CH11466. This work was also supported in part by the U.S. DOE under the Science Undergraduate Laboratory Internships (SULI) Program at General Atomics

Disclaimer: This report was prepared as an account of work sponsored by an agency of the United States Government. Neither the United States Government nor any agency thereof, nor any of their employees, makes any warranty, express or implied, or assumes any legal liability or responsibility for the accuracy, completeness, or usefulness of any information, apparatus, product, or process disclosed, or represents that its use would not infringe privately owned rights. Reference herein to any specific commercial product, process, or service by trade name, trademark, manufacturer, or otherwise does not necessarily constitute or imply its endorsement, recommendation, or favoring by the United States Government or any agency thereof. The views and opinions of authors expressed herein do not necessarily state or reflect those of the United States Government or any agency thereof.

[1] J. L. Luxon, Nuclear Fusion **42**, 614 (2002).

[2] P. B. Snyder, T. H. Osborne, K. H. Burrell, R. J. Groebner, A. W. Leonard, R. Nazikian, D. M. Orlov, O. Schmitz, M. R. Wade, and H. R. Wilson, Physics of Plasmas **19**, 056115 (2012).

[3] R. J. Groebner and S. Saarelma, Plasma Physics and Controlled Fusion **65**, 073001 (2023), publisher: IOP Publishing.

[4] R. C. Isler, Plasma Physics and Controlled Fusion **36**, 171 (1994).

[5] C. Chrystal, K. H. Burrell, B. A. Grierson, S. R. Haskey, R. J. Groebner, D. H. Kaplan, and A. Briesemeister, Review of Scientific Instruments **87**, 11E512 (2016), publisher: American Institute of Physics.

[6] T. N. Carlstrom, G. L. Campbell, J. C. DeBoo, R. Evanko, J. Evans, C. M. Greenfield, J. Haskovec, C. L. Hsieh, E. McKee, R. T. Snider, R. Stockdale, P. K. Trost, and M. P. Thomas, Review of Scientific Instruments **63**, 4901 (1992), publisher: American Institute of Physics.

[7] L. L. Lao, H. S. John, R. D. Stambaugh, A. G. Kellman, and W. Pfeiffer, Nuclear Fusion **25**, 1611 (1985).

[8] B. A. Grierson, K. H. Burrell, C. Chrystal, R. J. Groebner, D. H. Kaplan, W. W. Heidbrink, J. M. Muñoz Burgos, N. A. Pablant, W. M. Solomon, and M. A. Van Zeeland, Review of Scientific Instruments **83**, 10D529 (2012).

[9] S. R. Haskey, B. A. Grierson, L. Stagner, C. Chrystal, A. Ashourvan, A. Bortolon, M. D. Boyer, K. H. Burrell, C. Collins, R. J. Groebner, D. H. Kaplan, and N. A. Pablant, Review of Scientific Instruments **89**, 10D110 (2018), publisher: American Institute of Physics.

[10] B. A. Grierson, K. H. Burrell, C. Chrystal, R. J. Groebner, S. R. Haskey, and D. H. Kaplan, Review of Scientific Instruments **87**, 11E545 (2016).

[11] J. L. Luxon, M. J. Schaffer, G. L. Jackson, J. A. Leuer, A. Nagy, J. T. Scoville, and E. J. Strait, Nuclear Fusion **43**, 1813 (2003).

[12] P. C. Stangeby, J. M. Canik, J. D. Elder, C. J. Lasnier, A. W. Leonard, D. Eldon, M. A. Makowski, T. H. Osborne, and B. A. Grierson, Nuclear Fusion **55**, 093014 (2015), publisher: IOP Publishing.

[13] A. W. Leonard, A. G. McLean, M. A. Makowski, and P. C. Stangeby, Nuclear Fusion **57**, 086033 (2017), publisher: IOP Publishing.

[14] W. W. Heidbrink, D. Liu, Y. Luo, E. Ruskov, and B. Geiger, Communications in Computational Physics **10**, 716 (2011).

[15] B. Geiger, L. Stagner, W. W. Heidbrink, R. Dux, R. Fischer, Y. Fujiwara, A. V. Garcia, A. S. Jacobsen, A. J. v. Vuuren, A. N. Karpushov, D. Liu, P. A. Schneider, I. Sfiligoi, P. Z. Poloskei, and M. Weiland, Plasma Physics and Controlled Fusion **62**, 105008 (2020), publisher: IOP Publishing.

[16] I. H. Hutchinson, Plasma Physics and Controlled Fusion **44**, 71 (2002).

[17] D. N. Hill, Journal of Nuclear Materials **241-243**, 182 (1997).

[18] P. Virtanen, R. Gommers, T. E. Oliphant, M. Haberland, T. Reddy, D. Cournapeau, E. Burovski, P. Peterson, W. Weckesser, J. Bright, S. J. van der Walt, M. Brett, J. Wilson, K. J. Millman, N. Mayorov, A. R. J. Nelson, E. Jones, R. Kern, E. Larson, C. J. Carey, Polat, Y. Feng, E. W. Moore, J. VanderPlas, D. Laxalde, J. Perktold, R. Cimrman, I. Henriksen, E. A. Quintero, C. R. Harris, A. M. Archibald, A. H. Ribeiro, F. Pedregosa, and P. van Mulbregt, Nature Methods **17**, 261 (2020), number: 3 Publisher: Nature Publishing Group.